

Chemical Bonding, 10Dq Parameter and Superexchange in the Model Compound KNiF₃

Inés Sánchez-Movellán,^[a] José Antonio Aramburu,^{*[a]} and Miguel Moreno^[a]

The cubic field splitting parameter, 10Dq, plays a central role in the ligand field theory on insulating transition metal compounds. Experimental data obtained in the last 50 years prove that 10Dq is highly dependent on changes of the metal-ligand distance, R, induced by chemical or applied pressures. Despite this fact has important consequences on optical and magnetic properties of such compounds, its actual origin is still controversial. Seeking to clarify that crucial issue, this work is focused on KNiF₃, a reference system among insulating transition metal compounds. By means of first principles calculations we show that, contrary to what is usually thought, the R-dependence of 10Dq arises neither from the crystal field contribution nor from the covalent admixture of 3d(Ni) with valence 2p(F) orbitals. Indeed, we prove that it is mainly due to

the residual covalency with deep 2s(F) orbitals, highly sensitive to R variations. As a salient feature the present calculations show that the 3d–2pσ and 3d–2pπ admixtures raise practically equal the energy of antibonding e_g and t_{2g} orbitals of NiF₆^{4–} units in KNiF₃ thus leading to a null contribution to 10Dq. This conclusion is not significantly altered when considering the change of covalency on passing from the ground state ³A₂(t_{2g}⁶e_g²) to the excited state ³T₂(t_{2g}⁵e_g³). The different influence of chemical bonding on the superexchange constant, J, and 10Dq is also discussed in a second step. It is pointed out that the strong dependence of J upon R can hardly be explained through the behavior of the 3d–2pσ covalency derived for a single NiF₆^{4–} unit. For the sake of clarity, the meaning of 10Dq is also briefly analyzed.

1. Introduction

Significant research is currently devoted to exploring the properties of insulating Transition Metal (TM) compounds subject to a hydrostatic pressure.^[1–4] As a result of the electron localization in insulating lattices^[5] a good starting point for understanding the properties of TM compounds under pressure is just to consider the MX_N complex (M=TM cation, X=ligand) formed inside the lattice.^[6–8]

An applied pressure modifies the gap between the ground and excited states of the complex and it can even change their nature. For instance, in Na₃MnF₆ a pressure of only 2 GPa gives rise to a switch of the electronic ground state of MnF₆^{3–} units.^[9,10] As regards the CrF₆^{3–} complex in Cr³⁺-doped KZnF₃, the first excited state is ⁴T₂ at ambient pressure but becomes ²E for a pressure of about 8 GPa^[11] a situation also observed^[12] for K₂NaGaF₆:Cr³⁺. Along this line, an applied pressure on copper layered perovskites leads to a surprising red shift of some optical transitions.^[13]

The present work deals with pressure effects on model insulating compounds displaying cubic symmetry and involving octahedral TM complexes whose d-d transitions are described

in the approximate Tanabe-Sugano framework through the three B, C and 10Dq quantities.^[6,7] Interestingly, the two Racah parameters, B and C, of the MX₆ unit are systematically smaller than B₀ and C₀ corresponding to the free TM cation. This key fact is a direct result of the covalent bonding inside the MX₆ unit leading to unpaired electrons that spend some time on ligands.^[6,7,14,15]

The cubic field splitting quantity, 10Dq, reflects the gap between antibonding e_g and t_{2g} orbitals of the MX₆ unit. Indeed, the pioneering work by Sugano and Shulman^[16] on KNiF₃ already suggested that 10Dq mainly arises from the different chemical bonding involved in e_g and t_{2g} orbitals of the NiF₆^{4–} complex.

Nevertheless, although the three quantities B, C and 10Dq are all the result of the chemical bonding inside the MX₆ unit, they exhibit a very different response to pressure,^[11] a fact that is certainly puzzling. Indeed, while the Racah parameters are little sensitive to pressure, the 10Dq splitting is found to be greatly dependent upon the variations of the M–X distance, R, induced by hydrostatic or chemical pressures. In particular, experimental data are consistent with an expression 10Dq ∝ R^{–n} with the exponent n lying typically in the 4–6 range.^[4] This general pattern has been observed for ruby^[17,18] or along the series of cubic fluoroperovskites containing Mn²⁺ or Ni²⁺ cations, where the change of host lattice modifies the metal-ligand distance of involved MF₆^{4–} units (M=Mn, Ni).^[4,19–21]

Bearing these facts in mind, it has been put forward^[22,23] that the significant dependence of 10Dq upon R measured in KNiF₃ under pressure essentially arises from the crystal field contribution to 10Dq, termed (10Dq)_{CF}, as it is proportional to R^{–5}. Indeed (10Dq)_{CF} is given by the simple expression^[6,7] (–Z_Le = ligand charge)

[a] I. Sánchez-Movellán, J. A. Aramburu, M. Moreno
Departamento de Ciencias de la Tierra y Física de la Materia Condensada,
Universidad de Cantabria, Cantabria Campus Internacional, Avenida de los
Castros s/n, 39005 Santander, Spain
E-mail: aramburj@unican.es

© 2024 The Authors. ChemPhysChem published by Wiley-VCH GmbH. This is an open access article under the terms of the Creative Commons Attribution Non-Commercial NoDerivs License, which permits use and distribution in any medium, provided the original work is properly cited, the use is non-commercial and no modifications or adaptations are made.

$$(10Dq)_{CF} = \frac{5Z_L e^2}{3R^5} \langle r^4 \rangle_d \quad (1)$$

Nevertheless, in the case of octahedral TM complexes, Eq. (1) leads to 10Dq values clearly smaller than experimental ones using accurate values of $\langle r^4 \rangle_d$ corresponding to the free cation.^[4,19] Owing to these facts, the present work is aimed in a first step at clarifying the actual origin of 10Dq and its R-dependence in KNiF₃, a reference system among insulating transition metal compounds. In this study particular attention is paid to quantify the role played by chemical bonding. For achieving this goal, we explore in some detail, using first principles calculations, how covalency and 10Dq in KNiF₃ evolve when R is varied.

In complexes like MF₆⁴⁻ (M=Mn, Ni) embedded in insulating lattices, covalency essentially involves the admixture of 3d(M) levels with the valence 2p(F) levels^[7] of the fluorine ligand such as it is revealed by magnetic resonance data^[24-27] in systems like KNiF₃, KMnF₃, KMgF₃:Ni²⁺ or KZnF₃:Mn²⁺. For this reason, Anderson^[28] and also Owen and Thornley^[29] assumed that 10Dq primarily comes from the 3d(M)-2p(F) admixture on such complexes. Concerning the 2s(F) levels in such complexes, they are rather deep, as they lie ~23 eV below the 2p(F) levels just reflecting the situation already found in the free F and F⁻ species.^[4,8] Despite this fact, there is some *residual covalency* in MF₆⁴⁻ complexes (M=Mn, Ni) arising from the 3d(M)-2s(F) hybridization well detected through magnetic resonance measurements in pure and doped compounds.^[21,24-27,29,30] Interestingly, as this residual covalency is strongly dependent upon R for MnF₆⁴⁻ or NiF₆⁴⁻ units in cubic fluorides,^[30,21] it has been suggested that the 3d(M)-2s(F) admixture is the main source for 10Dq and its dependence upon R.^[31,32] Nevertheless, that conclusion seems to be at variance with the origin of the antiferromagnetic coupling in cubic perovskites like KNiF₃ or KMnF₃. Indeed, according to the results by Anderson, the antiferromagnetism in such lattices is mainly driven by the covalent admixture of 3d orbitals with the valence 2p(F) levels while the hybridization with deeper 2s(F) orbitals plays a minor role.^[28,29]

Seeking to shed light on this puzzling situation this work is firstly addressed to clarify how the covalency with 2p and 2s ligand levels evolves with pressure in KNiF₃ and KMgF₃:Ni²⁺, a crucial issue not well investigated up to now in these reference systems. Aside from exploring their influence upon 10Dq, we also examine whether the calculated 2p covalency in the single NiF₆⁴⁻ unit can account for the big dependence^[33] upon R of the antiferromagnetic exchange constant measured in KNiF₃.

The present work is organized as follows. For the sake of clarity, the theoretical grounds needed for the present analysis are shortly reviewed in section 2. In addition to recall the different contributions to 10Dq particular attention is paid to show how a weak covalent bonding can influence the 10Dq value. The computational tools used in the present study are described in detail in section 3, while main results obtained in this work on the reference systems KNiF₃ and KMgF₃:Ni²⁺ are

reported in section 4. Some final remarks are provided in the last section.

2. The Meaning of 10Dq: Influence of Chemical Bonding

In the case of octahedral TM complexes in insulating lattices, 10Dq appears as a central piece in the approximate description of multiplets.^[6,7] If the MX₆^{-q} complex (X=F, Cl, O, ...) involves a 3d^N cation, 10Dq is just equal to the energy difference $\epsilon(e_g) - \epsilon(t_{2g})$, corresponding to the two e_g and t_{2g} antibonding orbitals, which is obtained from the one electron Hamiltonian, h. By contrast, for calculating the energy of different electronic states it is also necessary to include the effects of the interelectronic repulsion, e²/r_{ij}. In the approximate Tanabe-Sugano framework, the multiplets are calculated considering only the e_g^mt_{2g}ⁿ (m+n=N) configurations, thus neglecting the influence of higher configurations (such as those arising from 3d^{N-1}4s¹) on the energy of states.^[6,7] This approximation is thus similar to that employed in the Slater's description of multiplets in free TM ions.^[34] Accordingly, for any of the e_g^mt_{2g}ⁿ (m+n=N) involved configurations the value 10Dq=E(e_g)-E(t_{2g}) is taken to be the same.

Within this approximation, the energy of different e_g^mt_{2g}ⁿ (m+n=N) states is calculated as a function of 10Dq and the ten independent Coulomb (J) and exchange (K) integrals^[6,7] associated with the e_g and t_{2g} molecular orbitals of the MX₆^{-q} complex (X=F, Cl, O, ...), that can briefly be written as^[7]

$$\begin{aligned} |e_g, u\rangle &= N_e \{ |3z^2-r^2\rangle - \lambda_\sigma |\chi_{p\sigma}(u)\rangle - \lambda_s |\chi_s(u)\rangle \} \\ |e_g, v\rangle &= N_e \{ |x^2-y^2\rangle - \lambda_\sigma |\chi_{p\sigma}(v)\rangle - \lambda_s |\chi_s(v)\rangle \} \\ |t_{2g}, \zeta\rangle &= N_t \{ |xy\rangle - \lambda_\pi |\chi_{p\pi}(\zeta)\rangle \} \\ |t_{2g}, \xi\rangle &= N_t \{ |yz\rangle - \lambda_\pi |\chi_{p\pi}(\xi)\rangle \} \\ |t_{2g}, \eta\rangle &= N_t \{ |xz\rangle - \lambda_\pi |\chi_{p\pi}(\eta)\rangle \} \end{aligned} \quad (2)$$

In short $|\chi_{p\sigma}(u)\rangle$ and $|\chi_s(u)\rangle$ stand for normalized linear combinations of the p_σ and s ligand valence orbitals, respectively, transforming like 3z²-r² under O_h symmetry. For the sake of clarity, the form of $|e_g, u\rangle$ is depicted in Figure 1, while the expressions of $|\chi_{p\sigma}(u)\rangle$, $|\chi_s(u)\rangle$, $|\chi_{p\sigma}(v)\rangle$, and $|\chi_{p\pi}(\zeta)\rangle$ are reported in Table 1.

Table 1. Expressions of $|\chi_{p\sigma}(u)\rangle$, $|\chi_s(u)\rangle$, $|\chi_{p\sigma}(v)\rangle$ and $|\chi_{p\pi}(\zeta)\rangle$ functions in terms of 2p and 2s atomic orbitals of individual ligand fluorine ions. The position of six ligands is described in Figure 1. A function like $|p_\sigma(5)\rangle$ is directed towards the origin of coordinates and transforms like $-(z-R)$ where R is just the metal ligand distance.

Function	Combination of ligands
$ \chi_{p\sigma}(u)\rangle$	$(1/\sqrt{12})[2(p_\sigma(5)\rangle + p_\sigma(6)\rangle) - (p_\sigma(1)\rangle + p_\sigma(2)\rangle + p_\sigma(3)\rangle + p_\sigma(4)\rangle)]$
$ \chi_s(u)\rangle$	$(1/\sqrt{12})[2(s(5)\rangle + s(6)\rangle) - (s(1)\rangle + s(2)\rangle + s(3)\rangle + s(4)\rangle)]$
$ \chi_{p\sigma}(v)\rangle$	$(1/2)[p_\sigma(1)\rangle - p_\sigma(2)\rangle + p_\sigma(3)\rangle - p_\sigma(4)\rangle]$
$ \chi_{p\pi}(\zeta)\rangle$	$(1/2)[p_y(1)\rangle + p_x(2)\rangle - p_y(3)\rangle - p_x(4)\rangle]$

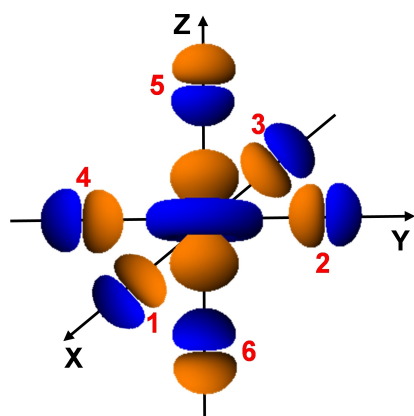


Figure 1. Picture of the antibonding $|e_g, u\rangle \sim 3z^2 - r^2$ molecular orbital for an octahedral NiF_6^{4-} unit in KNiF_3 cubic perovskite.

The transfer of the electronic charge from a 3d metal orbital to p_σ , s and p_π ligand orbitals is reflected by the q_σ , q_s and q_π quantities, respectively, defined by

$$q_\sigma = N_e^2 \lambda_\sigma^2 \quad q_s = N_e^2 \lambda_s^2 \quad q_\pi = N_t^2 \lambda_\pi^2 \quad (3)$$

Taking as a guide the ${}^3A_2(t_{2g}^6 e_g^2) \rightarrow {}^3T_2(t_{2g}^5 e_g^3)$ transition of an octahedral NiF_6^{4-} complex in KNiF_3 , its energy, $E({}^3A_2 \rightarrow {}^3T_2)$, within the present framework is approximated by^[7]

$$E({}^3A_2 \rightarrow {}^3T_2) = 10Dq + \{J(\zeta; u) - J(v; u)\} - \{K(\zeta; u) - K(v; u)\} \quad (4)$$

For obtaining the usual expressions of optical transitions of octahedral TM complexes, a further approximation is still

needed that implies to reduce the number of independent Coulomb and exchange integrals from ten to two.^[7] In that process $|e_g, u\rangle$ and $|t_{2g}, \zeta\rangle$ are taken simply equal to $|3z^2 - r^2\rangle$ and $|xy\rangle$, respectively, an approximation that is more reliable when covalency is reduced and thus more reasonable if the ligand is fluorine than bromine.^[14,8] On this basis, as $J(xy; 3z^2 - r^2) = J(x^2 - y^2; 3z^2 - r^2)$ and $K(xy; 3z^2 - r^2) = K(x^2 - y^2; 3z^2 - r^2)$, then the experimental value $E({}^3A_2 \rightarrow {}^3T_2) = 0.95 \text{ eV}$,^[7,20] yields the value of $10Dq$ for the octahedral NiF_6^{4-} complex in KNiF_3 within the approximated scheme developed by Tanabe and Sugano.^[7]

The influence of chemical bonding upon the gap between e_g and t_{2g} antibonding orbitals of an isolated O_h NiF_6^{4-} complex is described in two steps^[32] (depicted in Figure 2):

Step 1: We start considering the Ni^{2+} cation whose eight valence electrons are allowed to feel only the electrostatic potential, $V_{CF}(r)$, created by the six ligands taken as point charges. As this potential exhibits O_h symmetry, the energy of $e_g(3z^2 - r^2, x^2 - y^2)$ and $t_{2g}(xy, xz, yz)$ orbitals is equal to $E_{e_0} = E_d + \epsilon_e^{CF}$ and $E_{t_0} = E_d + \epsilon_t^{CF}$, where $2\epsilon_e^{CF} + 3\epsilon_t^{CF} = 0$ and E_d is the energy of the barycenter of five 3d levels. The difference $\epsilon_e^{CF} - \epsilon_t^{CF}$ is just the crystal field contribution to $10Dq$, termed $(10Dq)_{CF}$ in Eq. (1). Similarly, for a ligand of the NiF_6^{4-} complex, the corresponding $V_{CF}(r)$ potential breaks the degeneracy between $2p_\sigma$ and $2p_\pi$ orbitals as shown on the right side of Figure 2.

Step 2: We allow the hybridization of pure 3d orbitals with the corresponding ligand wavefunctions described by Eq. (1). In cases of low covalency ($N_e^2 \lambda_\sigma^2 \ll 1$ and $N_t^2 \lambda_\pi^2 \ll 1$), such as it happens for fluorides,^[8,14,29,35] the coefficients $N_e \lambda_\sigma$, $N_e \lambda_s$ and $N_t \lambda_\pi$ of antibonding orbitals can be expressed as^[32]

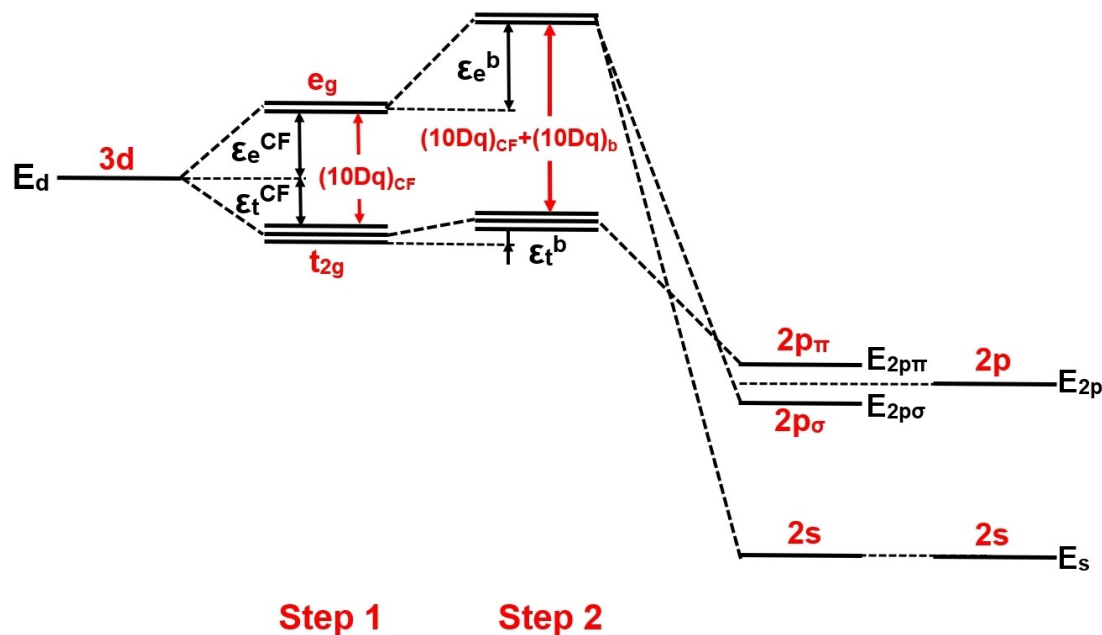


Figure 2. Qualitative scheme (not to scale) of the two contributions to the splitting $10Dq$ of 3d levels in KNiF_3 . Step 1 consider the Crystal-Field contribution $(10Dq)_{CF}$ of ligands and Step 2 the contribution $(10Dq)_b$ corresponding to the bonding between 3d orbitals of Ni (left side) and 2s and 2p orbitals of F (right side).

$$\begin{aligned}
 N_e \lambda_{\sigma} &= \langle 3z^2 - r^2 | h - E_{e0} | \chi_{p\sigma}(u) \rangle / (E_{e0} - E_{2p\sigma}) \\
 N_e \lambda_s &= \langle 3z^2 - r^2 | h - E_{e0} | \chi_s(u) \rangle / (E_{e0} - E_{2s}) \\
 N_t \lambda_{\pi} &= \langle xy | h - E_{t0} | \chi_{p\pi}(\zeta) \rangle / (E_{t0} - E_{2p\pi})
 \end{aligned} \quad (5)$$

Here h is the one electron Hamiltonian while $E_{2p\sigma}$ and E_{2s} are the energies of $2p\sigma$ and $2s$ ligand orbitals in the complex (Figure 2). As $E_{2p} - E_{2s} = 23$ eV for free F^- ,^[8] it can be expected $\lambda_{\sigma}^2 \gg \lambda_s^2$.

As a result of the formation of antibonding orbitals, there is also an additional energy raising for both e_g and t_{2g} orbitals (Figure 2). Calling ε_e^b and ε_t^b the corresponding increase due to chemical bonding, such quantities are well approximated when covalency is low by

$$\begin{aligned}
 \varepsilon_e^b &= N_e^2 [\lambda_{\sigma}^2 (E_{e0} - E_{2p\sigma}) + \lambda_s^2 (E_{e0} - E_{2s})] \\
 \varepsilon_t^b &= N_t^2 \lambda_{\pi}^2 (E_{t0} - E_{2p\pi})
 \end{aligned} \quad (6)$$

Bearing in mind that $E_{e0} - E_{t0}$ and $E_{2p\sigma} - E_{2p\pi}$ are around 0.1 eV and $10Dq \sim 1$ eV, the contribution to $10Dq$ arising from bonding in an isolated NiF_6^{4-} complex, $(10Dq)_b$ (Figure 2) can be approximated by the sum of contributions involving the covalency with $2p$ and $2s$ ligand orbitals

$$\begin{aligned}
 (10Dq)_b &= (10Dq)_{b,p} + (10Dq)_{b,s} \\
 (10Dq)_{b,p} &= (E_d - E_{2p})(N_e^2 \lambda_{\sigma}^2 - N_t^2 \lambda_{\pi}^2) = \\
 &= (E_d - E_{2p})(q_{\sigma} - q_{\pi}) \\
 (10Dq)_{b,s} &= \lambda_s^2 N_e^2 (E_d - E_{2s}) = (E_d - E_{2s}) q_s
 \end{aligned} \quad (7)$$

It is worth noting that, as TM complexes are embedded in insulating lattices, there is another contribution to $10Dq$ associated with the electric field $E_{ext}(r)$ created by the rest of lattice ions on the electrons confined in the complex.^[4] If this extrinsic contribution is termed $(10Dq)_{ext}$ the final $10Dq$ value can be expressed as

$$10Dq = (10Dq)_{CF} + (10Dq)_b + (10Dq)_{ext} \quad (8)$$

For a normal cubic perovskite as $KNiF_3$ or $KMgF_3$, the electric field $E_{ext}(r)$ is very flat along all directions of the MF_6 ($M = Ni, Mg$) octahedra.^[4,16,36] Therefore, in these materials, the step 3 corresponding to this extrinsic contribution $(10Dq)_{ext}$ is negligible and it is not considered in Figure 2.

It is worth noting that this $(10Dq)_{ext}$ contribution plays an important role in many other insulating materials, such as $LiBaF_3$ displaying the inverse perovskite structure. Indeed, the R distance is the same for $KMgF_3:M^{2+}$ and $LiBaF_3:M^{2+}$ ($M = Ni, Mn$), but $10Dq$ is about 0.1 eV higher for the second case as a result of the extrinsic contribution in the inverse perovskite structure.^[36–39] In the same vein, in $Al_2O_3:Cr^{3+}$ (ruby gemstone) and $Be_3Si_6Al_2O_{18}:Cr^{3+}$ (emerald) the $Cr^{3+} - O^{2-}$ distance is the same but the extrinsic contribution in ruby is 0.24 eV and basically responsible for the distinct color displayed by ruby and emerald.^[40–44]

Therefore, as it was already pointed out by Sugano and Shulman^[16] for a normal perovskite, the experimental $10Dq$ value for $KNiF_3$ should mainly arise from $(10Dq)_b$ reflecting the chemical bonding. Indeed, if we use the values $\langle r^4 \rangle = 3.16$ au^[45] for free Ni^{2+} , $R = 2.0$ Å and $Z_L = 0.90$ in Eq. (1), we obtain $(10Dq)_{CF} = 0.16$ eV, a value well below the experimental $10Dq = 0.95$ eV measured^[7,20,21] for both $KNiF_3$ and $KMgF_3:Ni^{2+}$.

At this point it is thus crucial to determine the weight of two contributions, $(10Dq)_{b,p}$ and $(10Dq)_{b,s}$, coming from bonding, to the final $10Dq$ value. Some information on the actual values of q_{σ} and q_s for the ground state of NiF_6^{4-} can be obtained from magnetic resonance measurements performed either on $KNiF_3$ or on $KMgF_3:Ni^{2+}$ ($M = Mg, Zn$).^[21,24–27] Nonetheless, as in the ground state of a NiF_6^{4-} complex there are no unpaired t_{2g} electrons, no information can be derived on the actual value of the $q_{\sigma} - q_{\pi}$ quantity and thus on the real weight of the $(10Dq)_{b,p}$ contribution to $10Dq$. This fact already stresses the importance of first principles calculations for clarifying that crucial issue in the model system $KNiF_3$.

3. Computational Tools

First-principles Density Functional Theory (DFT) calculations were carried out on Ni^{2+} -doped $KMgF_3$ and pure $KNiF_3$ compounds through periodic simulations using the CRYSTAL17^[46,47] code. Initially, we optimized the geometry of both systems, obtaining accurate results with errors of less than 1%. For $KNiF_3$, we employed the PW1PW^[48] hybrid functional, which includes 20% of exact Hartree-Fock exchange along with the high-quality all-electron triple-zeta polarized basis sets developed by Peitinger et al.^[47,49] In the case of $KMgF_3$ and Ni^{2+} -doped $KMgF_3$, the B1WC^[50] hybrid functional (with 16% of exact HF exchange) and the previous basis set were used. Results were cross verified with other hybrid functionals and basis sets, providing similar values. A $\sqrt{2} \times \sqrt{2} \times \sqrt{2}$ supercell was employed in $KNiF_3$ to accommodate the AFM-G order, while $2 \times 2 \times 2$ (40 ions) and $3 \times 3 \times 3$ (135 ions) supercell were used for $KMgF_3:Ni^{2+}$ system, both yielding comparable results.

Given that these systems are ionic compounds, our periodic calculations reveal that the active d-d electrons of Ni^{2+} ions are highly localized within the NiF_6^{4-} complex. Consequently, we performed cluster calculations using the Amsterdam Density functional (ADF) code,^[51] at the experimental and calculated geometries of $KNiF_3$ and $KMgF_3:Ni^{2+}$ respectively, in order to determine the value of the cubic field splitting $10Dq$ (Table 2). In the realm of the DFT, the value of $10Dq$ for a NiF_6^{4-} complex can be derived as the difference of the Kohn-Sham eigenvalues associated with e_g and t_{2g} orbitals but calculated for an artificial configuration where all one-electron orbitals (including the spin) are equally populated with 8/10 electrons. This procedure, related to the Slater's transition state,^[52] is explained in the paper by Adachi et al.^[53] Additionally, we computed the transfer of electronic charge from 3d metal orbital to ligand orbitals, denoted as q_{σ} , q_{π} and q_s , setting the open shell electronic configuration. These results, collected in Table 2, were derived from the Mulliken populations of the molecular orbitals. In a

Table 2. Values of 10Dq and covalency quantities obtained in the present work for both KNiF₃ and KMgF₃:Ni²⁺ compounds at ambient pressure through an all-electron calculation where core electrons are explicitly included. They are compared to experimental quantities (in italic letters) obtained from NMR and EPR measurements for such systems and also to those determined for KZnF₃:Ni²⁺ by ENDOR and CsCdF₃:Ni²⁺ by means of EPR. The values of the metal ligand distance, R, for KZnF₃:Ni²⁺ and CsCdF₃:Ni²⁺ are taken from Ref. [21]. The Ni²⁺-F⁻ distance, R, for KMgF₃:Ni²⁺ is calculated in this work.

System	R(Å)	10Dq (eV)	q _σ (%)	q _π (%)	q _s (%)	Ref.
KNiF ₃	2.006	0.96	14.22	15.14	2.83	
		<i>0.95</i>	<i>14.85 ± 1.8</i>	–	<i>1.5 ± 0.15</i>	20,24,25,55
KMgF ₃ :Ni ²⁺	1.996	0.98	14.21	15.12	2.87	
		<i>0.95</i>	<i>13.53 ± 0.45</i>	–	<i>1.5 ± 0.01</i>	20,26,29,35
KZnF ₃ :Ni ²⁺	2.01	<i>0.95</i>	<i>13.52</i>	–	<i>1.7</i>	27,56,31
CsCdF ₃ :Ni ²⁺	2.06	<i>0.77</i>	<i>12.7</i>	–	<i>1.35</i>	21

subsequent step, we explored the dependence of both 10Dq and q_σ, q_π and q_s on the metal-ligand distance, R. The outcomes of these analyses are discussed in section 4.2.

In these cluster calculations, we employed the widely used B3LYP hybrid functional^[54] (25% of HF exchange) and all-electron triple-zeta polarized basis sets included in the ADF package.^[48] We confirmed that similar trends were observed when larger clusters (up to 25 ions), different basis sets (DZP, augmented-TZP) and other functionals were considered. Furthermore, we have also performed all electron calculations where core electrons are explicitly included. We have verified that the different calculations carried out in this work lead to similar results. The internal electric field E_{ext}(r), generated by the rest of lattice ions has been included into these calculations via a classical embedding of point charges, previously obtained through Ewald-Evjen summations.^[39] However, in the normal perovskites, the effect of the internal electric field is negligible, as the electrostatic potential is fairly flat along the metal-ligand direction,^[4,16] and therefore, it exerts no significant influence on the results.

4. Results and Discussion

4.1. 10Dq and Covalency for KNiF₃ and Doped Fluoroperovskites at Ambient Pressure

The results of present calculations carried out for both KNiF₃ and KMgF₃:Ni²⁺ are displayed in Table 2 together with the corresponding experimental values^[24–26,29,35,55] as well as those measured for KZnF₃:Ni²⁺^[27,56,21] and CsCdF₃:Ni²⁺.^[21] Among doped systems, only in the case of KZnF₃:Ni²⁺ the super-hyperfine tensor has been measured through the electron nuclear double resonance (ENDOR) technique^[27] that helps to reach more accurate values of quantities q_σ = N_e²λ_σ² and q_s = N_e²λ_s² reflecting the covalency.

The calculated 10Dq values for KNiF₃ and KMgF₃:Ni²⁺ (Table 2) are the same and reasonably close to the experimental value of 0.95 eV.^[20] Such a table also shows that q_σ, reflecting the 3d–2pσ admixture, is clearly higher than q_s associated with the covalency with the deeper 2s(F) level. Moreover, the calculated q_σ quantity for KNiF₃ and KMgF₃:Ni²⁺ is in reasonable agreement with the experimental values.

As a salient feature, the values of the q_π quantity calculated in the present work for KNiF₃ and KMgF₃:Ni²⁺ are essentially coincident with q_σ. Therefore, this important fact strongly suggests that, according to Eq. (7), the contribution (10Dq)_{b,p} coming from the 3d–2pσ and 3d–2pπ covalent admixtures, actually plays a minor role for explaining the 10Dq value. This conclusion is consistent with magnetic resonance data for fluoroperovskites containing octahedral MnF₆^{4–} units involving both unpaired 2pσ and 2pπ electrons and a divalent cation.^[24,26,27,29,35] In that system, whose ground state is ⁶A₁(t_{2g}³e_g²), we can extract the quantity f_σ–f_π from the analysis of the ligand hyperfine tensor where the relation with the q_σ = N_e²λ_σ² and q_π = N_t²λ_π² quantities is just given by^[24,26,27,29,35]

$$f_{\sigma} = q_{\sigma}/3 \quad f_{\pi} = q_{\pi}/4 \quad (9)$$

A value f_σ–f_π = (0.18 ± 0.1)% has been derived from nuclear magnetic resonance (NMR) data for KMnF₃^[24] while from electron paramagnetic resonance (EPR) data on KMgF₃:Mn²⁺ it has been reported^[26] f_σ–f_π = (0.3 ± 0.5)%. Accurate ENDOR data^[27] on KZnF₃:Mn²⁺ lead to f_σ–f_π = 0.26%.

Therefore, in view of Eq. (8) and taking f_σ–f_π = 0.26%, we reach the conclusion that q_σ–q_π < 0.78% for MnF₆^{4–}. From the present calculations on KNiF₃, E_d–E_{2p} = 6 eV and thus, even assuming q_σ–q_π = 3%, the contribution (10Dq)_{b,p} would be around 0.2 eV and thus clearly smaller than the experimental value^[20] 10Dq = 0.95 eV. These data, together with Eqs. (6) and (7), thus support that the dominant contribution to 10Dq comes from the admixture of 3d orbitals with deep 2s ligand levels. As from the present calculations for KNiF₃, E_d–E_{2s} = 26 eV, then (10Dq)_{b,s} would be equal to 0.73 eV if q_s = 2.8% and equal to 0.45 eV if q_s = 1.7% (Table 2). The importance of the small 3d–2s hybridization is also underpinned looking at the dependence on the metal-ligand distance, R, of 10Dq and q_σ, q_π and q_s quantities describing the covalency. The results of that study are shown in the next section.

4.2. Dependence on R of 10Dq and Covalency Parameters

As expected, the R-dependence of calculated 10Dq and covalency parameters are practically identical for KNiF₃ and KMgF₃:Ni²⁺. Supporting this assertion, the calculated 10Dq

values at different metal-ligand distances are practically the same for both systems (Figure 3a). Moreover $10Dq$ is found to be sensitive to R and writing $10Dq \propto R^{-n}$ a value $n=4.90$ is obtained for KNiF_3 while $n=4.77$ for $\text{KMgF}_3:\text{Ni}^{2+}$. These values can be compared with $n=6.6 \pm 0.5$ measured for KNiF_3 under pressure^[23] and $n=5.4$ calculated for $\text{KZnF}_3:\text{Ni}^{2+}$.^[56] The comparison between experimental values at ambient pressure for $\text{KMgF}_3:\text{Ni}^{2+}$ ($10Dq=0.95$ eV and $R=2.00$ Å) and $\text{CsCdF}_3:\text{Ni}^{2+}$ ($10Dq=0.77$ eV and $R=2.06$ Å) (Table 2) also stresses the significant dependence of $10Dq$ upon R .

The evolution of N_e^2 and N_t^2 quantities and the covalent parameters q_σ and q_π for KNiF_3 calculated when the metal-ligand distance, R , is varied are displayed in Figure 3b and 3c, respectively. It should firstly be noticed that q_σ and q_π as well as N_e^2 and N_t^2 are found to be only slightly dependent on R . To be more specific, if $q_\sigma \propto R^{-n_\sigma}$ and $q_\pi \propto R^{-n_\pi}$, we obtain for KNiF_3 $n_\sigma = -0.02$ and $n_\pi = -0.6$. Therefore, this result points out that on the basis of Eq. (7), the significant dependence on R of $10Dq$ can hardly be ascribed to the $3d-2p$ admixture, a fact consistent with the main conclusion reached in section 4.1.

As shown in Figure 3d, the calculated behavior of q_s for KNiF_3 is quite different from that displayed by q_σ (Figure 3b) reflecting the covalency with $2p\sigma$ ligand levels. Indeed, the $3d-2s$ admixture is found to be highly dependent upon the metal-ligand distance, R , and writing $q_s \propto R^{-n_s}$, we obtain $n_s=6.93$. This fact is consistent with the decrease of q_s when comparing the values of $\text{KZnF}_3:\text{Ni}^{2+}$ ($q_s=1.7\%$ and $R=2.01$ Å) with $\text{CsCdF}_3:\text{Ni}^{2+}$ ($q_s=1.35\%$ and $R=2.06$ Å) derived from the experimental superhyperfine tensor (Table 2). The origin of the different R -dependence displayed by q_σ and q_s has previously been discussed in detail.^[4,30,32]

According to Eqs. (7) and (8) and the R -dependence of q_σ , q_π and q_s (Figure 3) and $(10Dq)_{CF}$ one can expect that if the $3d-2s$ admixture is the dominant contribution to $10Dq$ in KNiF_3 then it should be verified $n \leq n_s$. The present results are consistent with this inequality that is also verified by $10Dq$ and q_s values derived from experimental optical spectra and superhyperfine tensors for cubic fluoroperovskites containing MnF_6^{4-} units. In that series, it is obtained $n=4.8$ ^[57] while $n_s=7.8$.^[30] The calculated n and n_s values for the octahedral CrX_6^{3-} units ($X = \text{halide}$) fulfill the $n \leq n_s$ inequality as well.^[32]

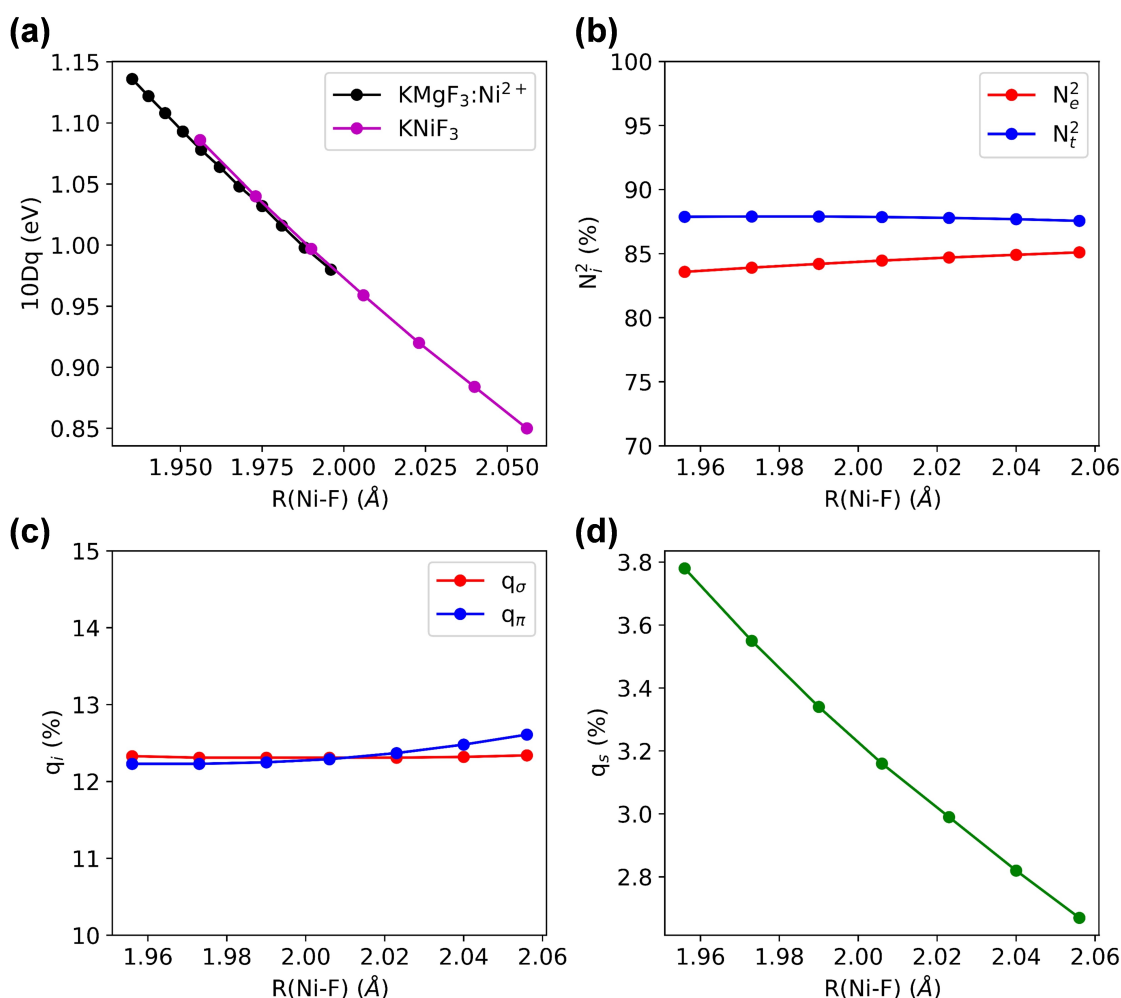


Figure 3. (a) Calculated dependence of the cubic-field splitting parameter $10Dq$ on the metal-ligand distance, R , for both KNiF_3 and $\text{KMgF}_3:\text{Ni}^{2+}$ systems. (b) Variation of N_e^2 and N_t^2 quantities with R calculated for KNiF_3 . (c) Calculated R dependence of q_σ and q_π for KNiF_3 . (d) Sensitivity of the residual density q_s to R changes derived for KNiF_3 .

4.3. Superexchange, Chemical Bonding and 10Dq: Further Questions

The present results on KNiF_3 strongly support that the sensitivity of 10Dq to R changes is actually driven by the big dependence of the small 3d–2s admixture in the antibonding e_g orbital. By contrast, the 3d–2p hybridization has a much smaller influence upon 10Dq as q_σ and q_π are essentially equal in the range $1.96 \text{ \AA} < R < 2.06 \text{ \AA}$ (Figure 3c).

By contrast, when we consider in KNiF_3 the exchange constant, J , between two closest Ni^{2+} ions, which share a F^- ion, there is an antiferromagnetic contribution, $J(\text{AFM})$, reflecting the chemical bonding of unpaired electrons. According to the model by Anderson^[28,29]

$$J(\text{AFM}) \propto (f_\sigma^*)^2 \quad (10)$$

where f_σ^* describes the σ covalency in the $\text{Ni}^{2+}\text{--F--Ni}^{2+}$ dimer. Therefore, at variance with what happens for 10Dq, $J(\text{AFM})$ for KNiF_3 is not dependent on f_π essentially because there are no π unpaired electrons in the ground state.

In his pioneering study on magnetic coupling in insulating compounds like KNiF_3 Anderson made two further assumptions^[28]

$$f_\sigma^* = f_\sigma \quad (11)$$

$$q_\sigma \gg q_\pi \quad (12)$$

Based on both assumptions and Eq. (7), then $J(\text{AFM})$ would be related to 10Dq of a single NiF_6^{4-} unit as follows

$$J(\text{AFM}) \propto (10\text{Dq})^2 \quad (13)$$

Although this expression suggests a strong dependence of $J(\text{AFM})$ upon R in KNiF_3 the calculated values in Figure 3 show that q_σ is practically equal to q_π and thus neither the assumption in Eq. (12) nor the conclusion of Eq. (13) are correct.

Experimental results on a variety of systems like KNiF_3 , RbNiF_3 , Ti_2NiF_4 or Rb_2NiF_4 show that the exchange constant, J , depends on R^{-p} with the exponent p lying in the 10–13 range.^[33] If this dependence is mainly due to the sensitivity of the antiferromagnetic contribution, $J(\text{AFM})$, to R changes further research is then necessary to understand its main origin. Indeed, if we only consider that $J(\text{AFM})$ depends on $(f_\sigma^*)^2$ (Eq. (9)) and also assume $f_\sigma^* = f_\sigma$ (Eq. (11)), it is hard to understand the experimental dependence of J upon R as the calculated $f_\sigma = q_\sigma/3$ is essentially independent on R such as it is shown in Figure 3.

5. Final Remarks

The present study carried out on the reference system KNiF_3 strongly supports that the crystal-field splitting parameter 10Dq mainly arises from the residual hybridization of 3d orbitals with deep 2s(F) ligand levels. This conclusion, suggested in previous

works on octahedral MnF_6^{4-} , CrF_6^{3-} or FeF_6^{3-} units,^[31,32,58] also stresses that the R-dependence of 10Dq is mainly due to the 3d–2s admixture, highly dependent upon R, and not to the crystal field contribution.

It should be noted that the condition $q_\sigma = q_\pi$ practically fulfilled for KNiF_3 is not necessarily followed in other TM complexes. For instance, in the O_h FeF_6^{3-} units formed in $\text{KMgF}_3:\text{Fe}^{3+}$ it has been derived from EPR measurements^[26,29,35] $f_\sigma - f_\pi = 3.3\%$ although the 3d–2s admixture has also been shown to be the main source of 10Dq.^[58]

The usual Tanabe-Sugano procedure assumes that the e_g and t_{2g} orbitals are frozen when considering the different $e_g^m t_{2g}^n$ ($m+n=8$) states of a NiF_6^{4-} unit.^[6,7] However, if we just consider the transition ${}^3A_2(t_{2g}^6 e_g^2) \rightarrow {}^3T_2(t_{2g}^5 e_g^3)$ the form of the two orbitals can change following the electron jump and thus the values of the charge transferred to ligands can in principle be different in the excited and in the ground state. Considering the three orbital states involved in the ${}^3T_2(t_{2g}^5 e_g^3)$ excited state, we have calculated the values $(q_\sigma)_{\text{ex}} = 16.7\%$, $(q_\pi)_{\text{ex}} = 11.7\%$ and $(q_s)_{\text{ex}} = 2.7\%$ corresponding to that mean excited state. If for describing the ${}^3A_2(t_{2g}^6 e_g^2) \rightarrow {}^3T_2(t_{2g}^5 e_g^3)$ transition we now use values of the three $(q_\sigma)_{\text{av}}$, $(q_\pi)_{\text{av}}$ and $(q_s)_{\text{av}}$ quantities that are the average between those for the ground (Table 1) and the excited state we obtain $(q_\sigma - q_\pi)_{\text{av}} = 2.1\%$ and $(q_s)_{\text{av}} = 2.8\%$. Therefore, these values again support that the 3d–2s admixture in KNiF_3 is the main source for 10Dq and its dependence upon the metal-ligand distance, R.

In CuF_6^{4-} units a tetragonal distortion produces a splitting of the e_g orbital into two singlet orbitals $a_{1g}(\sim 3z^2 - r^2)$ and $b_{1g}(\sim x^2 - y^2)$. The gap between them has also recently been shown to arise mainly from the different 3d–2s hybridization in the two orbitals once the distortion takes place while the 3d–2p admixture again plays a secondary role.^[59]

The results displayed in Figure 3 are also consistent with the highly different sensitivity to pressure 16% by 10Dq and the Racah parameters. Indeed, the experimental values found for KNiF_3 are $d10\text{Dq}/dP = 24 \text{ meV/GPa}$ while $dB/dP = -0.11 \text{ meV/GPa}$.^[23] As Coulomb and exchange integrals like $J(v; u)$ or $K(v; u)$ essentially depend on the probability of finding the two electrons on a metal orbital,^[60,15] then $J(v; u) \approx N_e^4 J(x^2 - y^2; 3z^2 - r^2)$ and $K(v; u) \approx N_e^4 J(x^2 - y^2; 3z^2 - r^2)$. Figure 3b shows that N_e^2 and N_t^2 are only slightly dependent upon R and thus qualitatively accounts for the small sensitivity of Racah parameters to pressure.

The study carried out in this work shows that, if we transfer the R-dependence of the f_σ quantity derived for a single NiF_6^{4-} unit (Figure 3c) to a $\text{Ni}^{2+}\text{--F--Ni}^{2+}$ dimer, it is in principle not easy to explain the big dependence on R of the exchange constant, J , found for KNiF_3 and other systems like RbNiF_3 , Ti_2NiF_4 or Rb_2NiF_4 or even in the pairs formed in highly doped samples of $\text{KMgF}_3:\text{Ni}^{2+}$.^[33] To answer this key question requires to study in detail the chemical bonding in the dimer following the way used in the analysis of K_2CuF_4 , K_2NiF_4 and Cs_2AgF_4 .^[61] Work along this line is now in progress.

Acknowledgements

The authors acknowledge financial support from Grant No. PID2022-139776NB-C63 funded by MCIN/AEI/10.13039/501100011033. I. S.-M. (grant BDNS:589170) acknowledges financial support from Universidad de Cantabria and Gobierno de Cantabria.

Conflict of Interests

The authors declare no conflict of interest.

Data Availability Statement

The data that support the findings of this study are available from the corresponding author upon reasonable request.

- [1] H. G. Drickamer, C. W. Frank, *Electronic Transitions and the High-Pressure Chemistry of Solids*, Chapman Hall, London, **1973**, pp. 72–109.
- [2] C. Reber, J. K. Grey, E. Lanthier, K. A. Frantzen, *Comm. on Inorg. Chem.* **2005**, *26*, 233–254.
- [3] L. K. Bray, *Top. Curr. Chem.* **2001**, *213*, 1.
- [4] M. Moreno, M. T. Barriuso, J. A. Aramburu, P. García-Fernández, J. M. García-Lastra, *J. Phys. Condens. Matter* **2006**, *18*, R315–R360.
- [5] W. Kohn, in *Many body physics*, (Eds.: C. deWitt, R. Balian R), Gordon and Breach, New York, **1968**, pp. 400–411.
- [6] J. S. Griffith, *The theory of transition-metal ions*, Cambridge, Cambridge, **1961** pp. 182–319.
- [7] S. Sugano, Y. Tanabe, H. Kamimura, *Multiplets of transition metal ions in crystals*, Academic Press: New York, **1970**, pp. 263–270, 126–153.
- [8] M. Moreno, J. A. Aramburu, M. T. Barriuso, *Struct. Bonding* **2004**, *106*, 127–152.
- [9] S. Carlson, Y. Xu, U. Halenius, R. Norrestam, *Inorg. Chem.* **1998**, *37*, 1486–1492.
- [10] I. Sánchez-Movellán, D. Carrasco-Busturia, J. M. García-Lastra, P. García-Fernández, J. A. Aramburu, M. Moreno, *Chem. Eur. J.* **2022**, *28*, e202200948.
- [11] P. T. C. Freire, O. Pilla, V. Lemos, *Phys. Rev. B* **1994**, *49*, 9232.
- [12] J. F. Dolan, A. G. Rinzler, L. A. Kappers, R. Bartram, *J. Phys. Chem. Solids* **1992**, *53*, 905–912.
- [13] D. Carrasco-Busturia, I. Sánchez-Movellán, A. S. Tygesen, A. Bhowmik, J. M. García-Lastra, J. A. Aramburu, M. Moreno, *Chem. Eur. J.* **2023**, *29*, e202202933.
- [14] C. K. Jørgensen, *Modern Aspects of Ligand Field Theory*, North Holland, Amsterdam, **1971**, pp. 293–313.
- [15] A. Trueba, J. M. García-Lastra, P. García-Fernández, J. A. Aramburu, M. T. Barriuso, M. Moreno, *J. Phys. Chem. A* **2011**, *115*(46), 13399–13406.
- [16] S. Sugano, R. G. Shulman, *Phys. Rev.* **1963**, *130*, 517–530.
- [17] S. Duclos, Y. K. Vohra, A. L. Ruoff, *Phys. Rev. B* **1990**, *41*, 5372–5381.
- [18] K. Syassen, *High Pressure Res.* **2008**, *28*, 75–126.
- [19] F. Rodríguez, M. Moreno, *J. Chem. Phys.* **1986**, *84*, 692–697.
- [20] K. Knox, R. G. Shulman, S. Sugano, *Phys. Rev.* **1963**, *130*, 512–516.
- [21] B. Villacampa, R. Cases, V. M. Orera, R. Alcalá, *J. Phys. Chem. Solids* **1994**, *55*, 263–272.
- [22] M. G. Brik, *Iop. Conf. Ser. Mater. Sci. Eng.* **2020**, *835*, 012032.
- [23] J. A. Barreda-Argüeso, F. Rodríguez, *Phys. Rev. B* **2021**, *103*, 085115.
- [24] R. G. Shulman, K. Knox, *Phys. Rev. Lett.* **1960**, *4*, 603–605.
- [25] R. G. Shulman, S. Sugano, *Phys. Rev.* **1963**, *130*, 506–511.
- [26] T. P. P. Hall, W. Hayes, R. W. H. Stevenson, J. Wilkens, *J. Chem. Phys.* **1963**, *38*, 1977–1984.
- [27] R. K. Jeck, J. J. Krebs, *Phys. Rev. B* **1972**, *5*, 1677–1687.
- [28] P. W. Anderson, *Solid State Phys.* **1963**, *14*, 99–214.
- [29] J. Owen, J. H. Thornley, *Rep. Prog. Phys.* **1966**, *29*, 675–728.
- [30] M. T. Barriuso, M. Moreno, *Phys. Rev. B: Condens. Matter Mater. Phys.* **1984**, *29*, 3623–3631.
- [31] M. Moreno, M. T. Barriuso, J. A. Aramburu, *Int. J. Quantum Chem.* **1994**, *52*, 829–835.
- [32] A. Trueba, P. García-Fernández, J. M. García-Lastra, J. A. Aramburu, M. T. Barriuso, M. Moreno, *J. Phys. Chem. A* **2011**, *115*, 1423–1432.
- [33] L. J. de Jongh, R. Block, *Physica B + C* **1975**, *79*, 568–593.
- [34] M. Tinkham, *Group Theory and Quantum Mechanics*, Mc Graw-Hill, New York, **1964**, pp. 154–178.
- [35] A. Abragam, B. Bleaney, *Electron paramagnetic resonance of transition ions*, Clarendon Press, Oxford, **1970**, pp. 761–784.
- [36] J. M. García-Lastra, J. Y. Buzaré, M. T. Barriuso, J. A. Aramburu, M. Moreno, *Phys. Rev. B* **2007**, *75*, 155101.
- [37] M. Mortier, B. Piriou, J. Y. Buzaré, M. Rousseau, J. Y. Gesland, *Phys. Rev. B* **2003**, *67*, 115126.
- [38] B. Henke, M. Secu, U. Rogulis, S. Schweizer, J. M. Spaeth, *Phys. Status Solidi C* **2005**, *2*, 380–383.
- [39] A. Trueba, J. M. García-Lastra, M. T. Barriuso, J. A. Aramburu, M. Moreno, *Phys. Rev. B: Condens. Matter Mater. Phys.* **2008**, *78*, 075108.
- [40] E. Gaudry, A. Kiratisin, P. Sainctavit, C. Brouder, F. Mauri, A. Ramos, A. Rogalev, J. Goulon, *Phys. Rev. B* **2003**, *67*, 094108.
- [41] E. Gaudry, D. Cabaret, C. Brouder, I. Letard, A. Rogalev, F. Wilhelm, N. Jaouen, P. Sainctavit, *Phys. Rev. B* **2007**, *76*, 094110.
- [42] J. A. Aramburu, P. García-Fernández, J. M. García-Lastra, M. T. Barriuso, M. Moreno, *Phys. Rev. B* **2012**, *85*, 245118.
- [43] J. A. Aramburu, P. García-Fernández, J. M. García-Lastra, M. T. Barriuso, M. Moreno, *J. Phys. Condens. Matter* **2013**, *25*, 175501.
- [44] M. O. J. Y. Hunault, Y. Harada, J. Miyawaki, J. Wang, A. Meijerink, F. M. F. de Groot, M. M. van Schooneveld, *J. Phys. Chem. A* **2018**, *122*, 4399–4413.
- [45] S. Fraga, J. Karwowski, K. M. S. Saxena, *Handbook of Atomic Data*, Elsevier, Amsterdam, **1976** p. 481.
- [46] R. Dovesi, A. Erba, R. Orlando, C. M. Zicovich-Wilson, B. Civalleri, L. Maschio, M. Rerat, S. Casassa, J. Baima, S. Salustro, B. Kirtman, *WIREs Comput. Mol. Sci.* **2018**, *8*, e1360.
- [47] CRYSTAL web page <http://www.crystal.unito.it/> access January 2023.
- [48] T. Bredow, A. R. Gerson, *Phys. Rev. B* **2000**, *61*, 5194–5201.
- [49] M. F. Peitinger, D. V. Oliveira, T. J. Bredow, *J. Comput. Chem.* **2013**, *34*, 451–459.
- [50] R. Shaltaf, G. M. Rignanese, J. Iniguez, D. I. Bilc, R. Orlando, Ph. Ghosez, *Phys. Rev. B* **2008**, *77*, 165107.
- [51] G. te Velde, F. M. Bickelhaupt, E. J. Baerends, C. F. Guerra, S. J. van Gisbergen, J. D. Snijders, T. Ziegler, *J. Comput. Chem.* **2001**, *22*, 931–967.
- [52] R. G. Parr, W. Yang, *Density-Functional Theory of Atoms and Molecules*, Oxford University Press, New York, **1989**, p. 141.
- [53] H. Adachi, S. Shiokawa, M. Tsukada, C. Satoko, S. Sugano, *J. Phys. Soc. Jpn.* **1979**, *47*, 1528–1537.
- [54] P. J. Stephens, F. J. Devlin, C. F. Chabalowski, M. J. Frisch, *J. Phys. Chem.* **1994**, *98*, 11623–11627.
- [55] D. Babel, A. Tressaud, in *Inorganic Solid Fluorides*, (Ed.: P. Hagenmuller), Academic Press, New York **1985**, p. 113.
- [56] M. G. Brik, G. A. Kumar, D. K. Sardar, *Mater. Chem. Phys.* **2012**, *136*, 90–102.
- [57] F. Rodríguez, M. Moreno, A. Tressaud, J. P. Chaminade, *Cryst. Lattice Defects Amorphous Mater.* **1987**, *16*, 221–225.
- [58] J. A. Aramburu, J. I. Paredes, M. T. Barriuso, M. Moreno, *Phys. Rev. B* **2000**, *61*, 6525–6534.
- [59] J. A. Aramburu, M. Moreno, *J. Phys. Chem. A* **2021**, *125*, 2284–2293.
- [60] D. Curie, C. Barthou, B. Canny, *J. Chem. Phys.* **1974**, *61*, 3048–3062.
- [61] I. Sánchez-Movellán, G. Santamaría-Fernández, P. García-Fernández, J. A. Aramburu, M. Moreno, *J. Phys. Chem. C* **2023**, *127*(33), 16695–16708.

Manuscript received: January 2, 2024
 Revised manuscript received: April 3, 2024
 Accepted manuscript online: April 4, 2024
 Version of record online: May 9, 2024